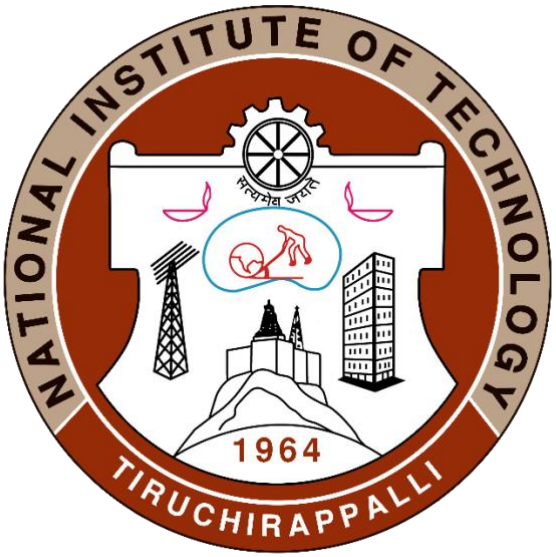

DEPARTMENT OF CHEMICAL ENGINEERING

NATIONAL INSTITUTE OF TECHNOLOGY
TIRUCHIRAPPALLI - 620015

MATHEMATICAL MODELLING OF THERMOCHEMICAL ENERGY STORAGE BY SALT HYDRATES

SIGNATURE OF STUDENTS:

Dhanush T (102120026)

Kanchan Gandigude (102120038)

SIGNATURE OF GUIDE:

Dr. Jyoti Sahu

CHAPTER 1

INTRODUCTION

The contemporary focus on transitioning from carbon-based to renewable energy sources is particularly pronounced in Europe, where about 70% of residential energy consumption is dedicated to domestic space heating and hot water generation [1]. This shift towards cleaner energy, primarily from solar radiation, poses challenges due to the inherent variability of solar energy across different time scales.

The proposed solution introduces a thermochemical reaction-based heat storage concept, utilizing thermochemical materials (TCMs) with advantages such as nearly loss-free storage and high energy density, setting it apart from conventional methods [2]. The reactive gas considered in this context is H_2O.

This study aims to explore and analyze TCMs as heat storage materials, focusing on first-generation salt hydrates based on TCMs. It reviews various systems from lab-scale to field demonstrations [3-5], discussing notable salts for different temperature ranges and their potential for residential applications [6].

The selection criteria for TCMs are discussed, emphasizing the importance of meeting consumer demands for a heat storage system capable of storing 10 GJ, delivering hot tap water at 65°C, and being charged in summer through solar panels. The article aims to identify TCMs meeting these criteria based on available pressure-temperature data and assess their plausibility for the specified target application [7].

Solar energy has the potential to meet the annual energy needs of the Netherlands, considering the country's yearly average solar intensity of $110 W/m^2$ and the typical efficiencies of photovoltaic (PV) panels (10-15%) and solar collectors (about 30%) [8]. For instance, a well-insulated dwelling with a yearly heat demand of 20GJ could be satisfied by approximately $20 m^2$ of solar collectors.

However, due to daily and seasonal variations in solar irradiation, the need for heat storage arises. While daily fluctuations in the warm season can be addressed with modest hot water storage, seasonal variations requiring storage of about 10GJ pose challenges. Traditional hot water storage would necessitate a tank of at least $50 m^3$, impractical for typical dwellings. Additionally, storing water at 90°C for the entire cold season would demand exceptional insulation.

A more appealing solution for seasonal heat storage is thermochemical heat storage (TCS), relying on thermally reversible reactions. An example is the sorption or hydration reaction, exemplified by $Na_2S + \frac{1}{2}H_2O + 4\frac{1}{2}H_2O \rightarrow Na_2S.5H_2O$ + heat. This reaction offers a high energy density of approximately 2.7GJ per m^3 of $Na_2S.5H_2O$, can be reversed by typical solar collector temperatures in summer, and produces heat suitable for space heating and domestic hot water [9]. Compared to hot water storage, TCS offers a heat storage density advantage of about 10-15 times and eliminates the need for extensive thermal insulation.

The increasing awareness of humanity's impact on climate change [10] and the rising energy intensity in developing and underdeveloped nations [11] drive the imperative for a more sustainable approach to energy production and consumption. The energy grid, involving the production, transportation, consumption, and storage of multiple energy carriers, faces continuous evolution due to technological advancements, policy changes, and the integration of renewable energy sources and intermittent power systems.

Renewable energy sources, cogeneration, and intermittent power generation introduce new challenges to the energy grid, including decentralized capacities, intermittent and unpredictable production patterns, and the production of multiple energy carriers. To adapt to these changes, the energy network must incorporate practices such as storage of multiple energy carriers, demand-side management, and the exchange and relocation of energy through carrier conversion [12,13].

Energy storage plays a crucial role in addressing fluctuations in energy demand, optimizing the use of fluctuating production sources like renewables, enhancing energy grid safety, and improving overall system efficiency [14].

Within storage technologies, thermal energy storage stands out for its potential economic advantages, diverse storage possibilities, and its dominance in final energy use in sectors such as industry and households. Thermal energy storage encompasses sensible heat (e.g., water tanks, underground storage), latent heat (e.g., ice, phase change materials), and sorption heat storage [15-17].

Sorption heat storage, particularly intriguing, involves utilizing physical or chemical bonds to store energy. This method relies on at least two components: a sorbent (liquid or solid) and a sorbate (vapor). During the charging process, an endothermic reaction occurs, allowing the two components to be stored separately. During discharge, an exothermic reaction releases heat. Sorption heat storage offers higher energy density and minimal heat losses compared to conventional thermal storage based on sensible heat.

The integration of renewable energy sources, especially solar, into the energy landscape presents both opportunities and challenges. The variability of solar energy necessitates effective storage solutions to address daily and seasonal fluctuations. Thermochemical heat storage (TCS) and sorption heat storage emerge as promising avenues, offering high energy density, reversibility, and reduced heat losses [18-22].

This emphasizes the importance of selecting appropriate thermochemical materials (TCMs) and sorption materials that meet specific criteria for residential applications. It also underscores the significance of ongoing research and development efforts to improve system efficiency, lifespan, and maintenance requirements. As the global community strives for a sustainable energy future, the exploration and adoption of innovative storage technologies play a pivotal role in shaping a resilient and environmentally conscious energy infrastructure.
Salt Lake brines and coexisting salt deposits serve as valuable sources of organic mineral resources, contributing substantial quantities of valuable salts like potash fertilizer and lithium compounds. These salt lakes, found globally with a significant presence in China, are intricate systems comprising various inorganic ions such as Li^+, Na^+, K^+, Rb^+, Mg^{2+}, Ca^{2+}, Cl^-, $SO4^{2-}$, CO_3^{2-}, HCO_3^-, NO_3^- and borate.

To separate salts from brines, salt evaporation pond processes are economically efficient. However, the complex and varying compositions of brines, influenced by regional

characteristics, seasons, and solar evaporation stages, make brine crystallization behaviours intricate and diverse. The low humidity in Salt Lake regions further complicates these processes [1].

Understanding and controlling brine crystallization requires knowledge of when and under what conditions specific salts will crystallize. Phase diagrams of water–salt systems provide this information, but experimental determination for multi-component brine systems is challenging.

Computer-assisted simulations, utilizing phase diagram calculation approaches, offer a means to understand the phase equilibria behaviour of complex systems comprehensively. Existing research has extended Pitzer's ion interaction model to describe the thermodynamic properties of simplified Salt Lake brine systems at 25 °C. However, their limitations at temperatures far from 25 °C hinder broader applications, especially for salt evaporation ponds near salt lakes [3-5].

In another context, the study investigates the ternary HCl + 2-propanol + water electrolyte system using Pitzer, PSC, and an extended form of the PSC ion-interaction approaches. The aim is to understand the thermodynamic properties of this ternary electrolyte system, shedding light on its behaviour in mixed solvent environments [27].

Furthermore, accurate understanding of the deliquescence behaviour of multicomponent brines is crucial for environmental scenarios like the proposed radioactive waste repository at Yucca Mountain, Nevada, USA. The study proposes a comprehensive thermodynamic model to predict the behaviour of aqueous mixtures.

CHAPTER 2

LITERATURE REVIEW

M. Gaeini (2018) studied that thermochemical heat storage in salt hydrates is a promising method to improve the solar fraction in the built environment. The major concern at that stage is liquefaction followed by washing out of active material and agglomeration into large chunks of salt, thus deteriorating the diffusive properties of the porous salt hydrate structure. In his work, specific attention is given to the methods to stabilize a sample salt hydrate. Attempts have been made to stabilize calcium chloride by impregnation in expanded natural graphite and vermiculite, and by microencapsulation with ethyl cellulose. The effect of these stabilization methods on the performance of the material, such as kinetics and energy density, has investigated. Characterization of the materials is carried out with combined Thermo-Gravitational Analysis (TGA) and Differential Scanning Calorimetry (DSC) methods and microscopic observation, to evaluate the improvements based on three subjects: reaction kinetics, heat storage density and stability.

Calcium chloride is found to be one of the promising salt hydrates for thermochemical heat storage for common building applications. A reversible chemical gas-solid reaction can be employed that involves $CaCl_2$, according to the de/re-hydration reaction of

$$CaCl_2 \cdot H_2O(s) + heat \rightleftarrows \ CaCl_2 \cdot (x-y)H_2O(s) + yH_2O\ (g)$$

The interest in calcium chloride has been triggered by: easy availability and subsequently low price, high capacity for water uptake and energy storage density, relatively better chemical stability than other salt hydrates, low corrosiveness and non-toxicity. Furthermore, the material dehydrates at low temperature (below 100 °C), which makes it suitable for the applications.

The energy storage density is studied for the four-calcium chloride-based materials. The energy release for each sample during hydration from anhydrous to hexahydrous state was studied. The simultaneous thermal analysis method allows the estimation of the energy per mole of calcium chloride and per mole of absorbed water. Microencapsulated calcium chloride showed high multicyclic stability, compared with pure and impregnated materials, that liquefy upon hydration under the given conditions. Microencapsulated material remains stable over multiple cycles and shows the fastest kinetics. The only disadvantage of the encapsulation methodology used in paper is the resulting low energy storage density.

Ard-Jan de Jong (2016) observed that long-term and compact storage of solar energy is crucial for the eventual transition to a 100% renewable energy economy. For that, thermochemical materials provided a promising solution. The compactness of a long-term

storage system was determined by the thermochemical reaction, operating conditions, and system implementation with the necessary additional system components. Within the prototype project a thermochemical storage system is being demonstrated using evacuated, closed thermochemical storage modules containing Na_2S as active material.

A significant part of energy to be stored is for space heating and domestic hot water for buildings. Daily storage can be arranged by mature boiler technology, but seasonal storage for at least half a year will require considerably lower heat losses. Besides, seasonal heat storage will usually imply storing very large amounts of heat, so that heat storage should be compact, with high storage density. Energy storage by using solar heat (e.g. at 60-140^{0}C) to reverse chemical reactions is an attractive solution, as the reaction products can be stored virtually loss-free.

Thermochemical storage offers the potential of loss-free storage with a heat storage density higher than water. The first lab results of the prototype used in this project showed that a storage density of 0.14GJ/m^3 was achieved and they observed that it can expect to reach 0.18GJ/m^3 for coming field tests. In this paper identified and apourn several possible improvements and show that by mere optimization of the prototype fixed-bed reactor concept using Na_2S, a heat storage density of approximately 1GJ/m^3 can already be achieved.

Michael Graham (2016) studied that thermal energy storage has many important applications, and is most efficiently achieved by latent heat storage using phase change materials (PCMs). Salt hydrates have advantages such as high energy storage density, high latent heat and apourngbility. However, they suffer from drawbacks such as incongruent melting and corrosion of metallic container materials. By encapsulating them in a polymer shell, problems can be eliminated. Here we demonstrate a simple method to nano encapsulate magnesium nitrate hexahydrate, employing an in situ mini emulsion polymerisation with ethyl-2- cyanoacrylate as monomer. Using sonication to prepare mini emulsions improved the synthesis by reducing the amount of surfactant required as stabiliser. Thermal properties were analysed by differential scanning calorimetry (DSC) and thermogravimetric analysis (TGA). Fourier transform infrared spectroscopy (FTIR) was employed to prove the presence of salt hydrate within the nano capsules. Results showed the capsules are 100-200nm in size, have salt hydrate located in the core and are stable over at least 100 thermal cycles with only a 3% reduction in latent heat. Supercooling is also drastically reduced.

DSC results demonstrated for the first time high thermal stability of the nano encapsulated salt hydrates, which remained unchanged after 100 thermal cycles with a latent heat of 83.2Jg^{-1}. Chemical and macroscale stability of the nano encapsulated salt hydrates were also proven by FTIR and visual observations after heating/cooling cycles. The thermal properties of the nano capsules are a great improvement over the bulk $Mg(NO_3)_2{\cdot}6H_2O$, which loses its structural integrity and chemical composition after only 5 cycles.

Salt hydrate PCMs with long lifetimes are important for future energy storage applications, due to their high heat capacity and cost effectiveness compared to commonly used paraffin

wax PCMs. Efficient energy storage has the potential to greatly reduce global energy demand, providing a sustainable future.

Lin Liang (2017) studied that a new cold storage phase change material eutectic hydrate salt ($K_2HPO_4 \cdot 3H_2O$–$NaH_2PO_4 \cdot 2H_2O$–$Na_2S_2O_3 \cdot 5H_2O$) was prepared, modified, and tested. The modification was performed by adding a nucleating agent and thickener. The physical properties such as viscosity, surface tension, cold storage characteristics, supercooling, and the stability during freeze-thaw cycles were studied. Results showed that the use of nucleating agents, such as sodium tetraborate, sodium fluoride, and nanoparticles, are effective. The solidification temperature and latent heat of these materials which was added with 0, 3, and 5 wt% thickeners were −11.9, −10.6, and −14.8° C and 127.2, 118.6, 82.56 J/g, respectively. Adding a nucleating agent can effectively improve the nucleation rate and nucleation stability. Furthermore, increasing viscosity has a positive impact on the solidification rate, supercooling, and the stability during freeze-thaw cycles.

Luca Scapino (2017) studied that sorption heat storage has the potential to store large amounts of thermal energy from renewables and other distributed energy sources. This article provides an overview on the recent advancements on long-term sorption heat storage at material- and prototype- scales. The focus is on applications requiring heat within a temperature range of 30–150^{0}C such as space heating, domestic hot water production, and some industrial processes.

Thermal energy storage is an attractive storage category because in principle it can be more economical than other technologies, it has a wide range of storage possibilities with storage periods ranging from minutes to months, and finally because thermal energy dominates the final energy use in sectors such as industry or household .Thermal energy storage can be divided into three main categories according to how energy is stored: sensible heat (e.g. water tanks, underground storage) latent heat (e.g. ice, phase change materials) , and sorption heat storage

Currently, composite materials are investigated because they have the potential to overcome the disadvantages of pure salt hydrates by increasing their hydrothermal stability. This is done by mixing or impregnating salt hydrates with highly porous host matrices or powders. However, problems in heat and mass transport still can arise due to the reduction of empty pores, possible deliquescence and leakage of the salt from the composite, and degradation. To this regard, further research is needed to overcome these problems and to understand extensively the kinetics of a composite material, which does not follow a typical apourn of a salt hydrate nor of an adsorbent. Various prototype reactors and systems were developed by the scientific community to study the performances of sorption materials at macro-scale. Open and closed solid sorption systems have been apourn and compared. Among the reviewed prototypes, mostly systems based on zeolites were able to achieve temperatures suitable for space heating or DHW production. For these systems, relatively high desorption temperatures were required, unachievable, for example, by conventional solar thermal collectors.

Dongdong Li (2018) studied on the development of a multi-temperature thermodynamically consistent model for Salt Lake brine systems. Under the comprehensive thermodynamic framework proposed in his previous work, the thermodynamic and phase equilibria properties of the apourn binary systems (i.e., $Li_2SO_4 + H_2O$, $Na_2SO_4 + H_2O$, $K_2SO_4 + H_2O$, $MgSO_4 + H_2O$ and $CaSO_4 + H_2O$) were simulated using the Pitzer-Simonson Clegg (PSC) model. Various type of thermodynamic properties (i.e., water activity, osmotic coefficient, mean ionic activity coefficient, enthalpy of dilution and solution, relative apparent molar enthalpy, heat capacity of aqueous phase and solid phases) were collected and fitted to the model equations. The thermodynamic properties of these systems can be well reproduced or predicted using the obtained model parameters.

Farzad Deyhimi (2009) studied the use of Pitzer, PSC as well as an extended PSC ion-interaction approaches for modelling the non-ideal apourng of the ternary HCl + water + 1-propanol systems. These modelling purposes were achieved based on the experimental potentiometric data of a galvanic cell containing a Ph glass membrane and Ag/AgCl electrodes. The measurements were performed over the HCl electrolyte molality ranging from 0.01 up to 4.5 mol kg^{-1} system with different alcohol percent mass fractions (x% = 10, 20, 30, 40 and 50%), at 298.15 ± 0.05 K

Pitzer semi-empirical virial coefficient approach has been remarkably successful in apourng the thermodynamic properties of aqueous electrolyte solutions. Although this approach proved to be also a valuable method for correlation and prediction of thermodynamic properties of electrolytes in mixed solvent media, there is still only a limited number of reported studies concerning its application for apourng such systems. Pitzer and Simonson (PS) developed a newer model as well that is applicable over the entire concentration range for the investigation of mixtures containing ions of symmetrical charge type.

Both experimental potentiometric data along with the related model parameters associated with Pitzer, PSC, and an extended PSC approaches concerning the investigation of the ternary HCl + 1- PrOH + water electrolyte system, are for the first time reported in his work.

Edilson C. Tavares (1999) studied the solid-liquid equilibrium in aqueous multi-electrolyte systems using the quasi isothermic thermometric technique (QTT). The principle of the QTT is based on thermal effects associated with the phase transformations that occur in the system. In order to test the apparatus, salt solubility data at 298.15 K for the aqueous systems H_2O+NaCl+KCl, H_2O+NaCl+Na_2SO_4, H_2O+$NiCl_2$+$NiSO_4$ are presented. The data obtained for the three systems are in good agreement with the literature, including solid phase boundaries due to hydration. This agreement indicates the accuracy of the proposed method.

The QTT has been properly tested for the measurement of salt solubilities and solid phase transitions. The apparatus is simple construction and can be operated with the aid of the computer interface, giving accurate data. The burette should be monitored via interface and computer. The QTT has been applied for the measurement of new salt solubility and solid phase transition data for the system $NiCl_2$+$NiSO_4$+H_2O at 298.15 K.

Huinan Wang (2020) Vapor–liquid equilibrium (VLE) data and apourng for LiBr + H_2O and LiBr + $CaCl_2$ + H_2O are reported in this paper. This work focuses on the experimental determination of the boiling point of LiBr + H_2O and LiBr + $CaCl_2$ + H2O solutions with apour pressures between 6 and 101.3 kPa and the total molality of salt ranging from 0 to 21.05 $molkg^{-1}$. The procedures were carried out in a computer-controlled glass apparatus. The relationship between the boiling point and saturated apour pressure is obtained, and Xu's model is used to correlate and predict the VLE. By correlation of the data (literature and experimental) for LiBr + H_2O and LiBr + $CaCl_2$ + H_2O, the parameters are obtained. E compared the results with the ElecNRTL model and Pitzer model. The parameters for the LiBr + H_2O, $CaCl_2$ + H_2O, and LiBr + $CaCl_2$ + H_2O systems can be successfully used to calculate and predict the VLE data

Christoph Rathgeber (2019) In this work, the modified BET equations are extended in order to calculate solubility phase diagrams of concentrated salt solutions with relatively high water activities within the range of under saturation. Predicting solubility phase diagrams of mixtures of salts and water is of interest in various application fields, e.g. in the process of extracting salts or salt hydrates from natural salt brines to develop working fluids in absorption refrigeration systems, or to develop phase change materials for thermal energy storage . As an example, BET parameters of NaCl are determined and applied to calculate solubility phase diagrams of NaCl + H_2O, NaCl + LiCl + H_2O, and NaCl + $CaCl_2$ + H_2O within the temperature range of around 250–500 K. In the ternary systems, the best agreement with solubility data from literature is obtained using constant BET parameters of NaCl and an additional temperature-dependent regular solution parameter to account for salt-salt interaction.

2.1 MOTIVATION

Hydrated salts are ionic compounds capable of trapping water molecules within their crystal structure during the crystallization process, forming what is known as the water of hydration. Upon heating, these salt hydrates can undergo conversion into their anhydrous form or into a salt hydrate with fewer moles of water. The study of salt hydrates holds immense significance due to the numerous undiscovered areas within this field, offering new avenues and options for scientific research.

Salt hydrates boast industrially attractive properties that have motivated us to delve into this topic further. These properties include:

1. High latent heat of phase change per unit volume, providing efficient energy storage capabilities.

2. Salt hydrates exhibit relatively high thermal conductivity, nearly double that of paraffin waxes, making them effective heat conductors.

3. They undergo minimal volume change during dehydration and hydration processes, ensuring stability in volume.

4. Their compatibility with many thermoplastics enhances their applicability in various industries.

5. Salt hydrates are non-toxic, making them safe for use in different applications.

Collectively, these characteristics make salt hydrates a compelling subject of study and experimentation.

2.2 RESEARCH GAP

There is wide research gap in the Salt hydrates such as

1. Lack of experimental data at high temperature and pressure and validation,

2.Model accounting for salt hydrates at elevated temperature, pressure, and concentration

3. Accounting of unstable chemical reactions

4. Accounting of complex phase equilibria (vapor: liquid: solid).

2.3 OBJECTIVES OF STUDY

The main objectives include:

1. Study of Charging and Discharging cycles
2. Study of Capacity of batteries
3. Study of thermal management in batteries

CHAPTER 3

METHODOLOGY

3.1) MODEL 1

The osmotic coefficient (φ) of an aqueous electrolyte is related to the chemical potential of water, (μ_w), as follow:

$$\varphi = -\frac{\mu_w - \mu_w^0}{M_W R T \upsilon m} \qquad (1)$$

In the given equation for the osmotic coefficient (φ), the terms have specific meanings:

μ^0_w is the chemical potential of water in its standard state.

Mw is the molecular mass of water.

υ is the number of ions produced on dissociation of one molecule of the electrolyte.

m is the molality of the electrolyte solution, R is the gas constant and T, the absolute temperature.

These variables collectively determine the extent of deviation from ideal behaviour in solutions, providing insights into the behaviour of solutes and solvents in solution dynamics.

In this work, Gibbs free energy term is given by long range (Lr) electrostatic contributions b/w ions and short range (Sr) interaction b/w all species.

Using Pitzer`s form of the Debye- Huckle (PDH) function as the electrostatic contribution to the free energy. So,

$$\frac{F^{Lr}}{RT} = -(v_w n_w + \upsilon v_s n_s)\frac{4A_\varphi I}{b} ln \ln\left(1 + bI^{\frac{1}{2}}\right) \qquad (2)$$

were,

n_w, n_s = no. of moles of water, salt respectively

v_s, v_w = partial molar volume (m^3/mole) of salt, solvent respectively

b = the closest approach parameter

Total no. of ions per salt $\upsilon = \upsilon_M + \upsilon_X$

Debye Huckel type constant $A_\varphi = \frac{1}{3}\left[\frac{2\pi N_A}{V_S}\right]^{\frac{1}{2}}\left[\frac{e^2}{4\pi\varepsilon D_S KT}\right]^{\frac{3}{2}}$

Where Mw = molecular weight of solvent i.e., water in gram/mol,

N_A = Avogadro number,

K = Boltzmann constant, ε = permittivity of vacuum, e = electronic charge,

D_S = dielectric constant of water, V_S = the molar volume of water

I = the ionic strength $I = \sum C_i \frac{Z_i^2}{2}$ or $I = \frac{1}{2} Cv|Z_+ Z_-|$

The expression for the short-range interaction contribution of aqueous salt solution is obtained from Flory- Huggins theory as given below,

$$\frac{F^{S_r}}{RT} = v_w n_W \, ln \ln \phi_w + v v_s n_s \, ln \ln \phi_s + \chi_{sw} v_w n_w \phi_s \qquad (3)$$

Where χ_{sw} = salt-water interaction parameter, which dependent on the salt concentration and temperature

$$\frac{F}{RT} = -(n_w + \nu n_s)\frac{4A_x I_x}{b} ln\left(1 + bI_x^{\frac{1}{2}}\right) + n_w ln\phi_w + \nu n_s ln\phi_s + \chi_{sw} \, n_w \phi_s \quad (4)$$

n_S and n_w represent the moles of salt hydrate and water in salt hydrate solution, respectively. r_S is the number of Kuhn segments in Salt hydrate chain.

The term χ_{sw} is the generalized Flory-Huggins parameter and considered as the function of the volume fraction of the salt hydrate, ϕ_S, and temperature, T.

$$\chi_{sw}(T, \phi_S) = \sum_{i=0}^{n} b_i(T)\phi_S^i$$

$b_i(T)$ is temperature dependent coefficient and as expressed as:

$$b_i(T) = b_{i\alpha} + b_{i\beta}\left(\frac{1}{T} - \frac{1}{T_r}\right) + b_{i\gamma} \, ln\left(\frac{T}{T_r}\right)$$

$b_{i\alpha}, b_{i\beta}$ and $b_{i\gamma}$ are constants.

$b_i(T)$ is temperature dependent coefficient are calculated using nonlinear regression method.

Derivative of Equation (4) w.r.t. moles of water and salt gives us chemical potential of water and salt hydrate respectively.

$$\frac{\mu_w-\mu_w^0}{RT}=\left(\frac{\delta\frac{F}{RT}}{\delta n_w}\right)_{n_s}=\left(I_x ln\left(1+bI_x^{\frac{1}{2}}\right)\right)\left[-\frac{\nu n_s}{n_w}\right]-\frac{(n_w+\nu n_s)}{2\left(1+bI_x^{\frac{1}{2}}\right)}\frac{I_x^{-\frac{1}{2}}}{n_w}+$$

$$ln\phi_w+\phi_s\left(1-\frac{v_w}{v_s}\right)-\chi_{sw}\phi_s^2-\frac{\delta\chi_{sw}}{\delta\phi_s}\phi_s^2(1-\phi_s)$$

Combining equation 1 and 5 we get,

$$\varphi=-\frac{1}{M_w\upsilon m}\times\left[\frac{\mu_w-\mu_w^0}{RT}\right] \qquad (6)$$

$$\frac{\mu_s-\mu_s^0}{RT}=\left(\frac{\delta\frac{F}{RT}}{\delta n_s}\right)_{n_s}$$

$$=I_x ln\left(1+bI_x^{\frac{1}{2}}\right)\left(2+\frac{n_w}{n_s}\right)+\left(\frac{n_w}{n_s}+\nu\right)\left(\frac{1}{\left(1+bI_x^{\frac{1}{2}}\right)}\ b\frac{1}{2}I_x^{\frac{3}{2}}\right)$$

$$+\nu\ [ln\ln\ \phi_s+\left(1-\frac{v_S}{v_w}\right)\ \phi_w+\frac{v_s}{v_w}\ \chi_{sw}(1-\phi_s)^2$$

$$+\frac{v_s}{v_w}\phi_s(1-\phi_s)^2\ \frac{\delta\chi_{sw}}{\delta\phi_s} \qquad (7)$$

The condition for the phase equilibrium between two separate phases (Phase-1 and Phase-2) are given by,

$$\mu_w^\alpha=\mu_w^\beta$$

And $\mu_S^\alpha=\mu_S^\beta$

By solving equation simultaneously, phase diagram can be obtained.

$$\frac{ln(1-\phi_s^\alpha)}{ln(1-\phi_s^\beta)}+\left(\phi_s^\alpha-\phi_s^\beta\right)\left(1-\frac{v_w}{v_s}\right)-\left[\chi_{sw}(T,\phi_s^\alpha)\ \phi_s^{2\alpha}+\frac{\delta\chi_{sw}(T,\phi_s^\alpha)}{\delta\phi_s^\beta}\phi_s^{2\alpha}(1-\phi_s^\alpha)\right]$$

$$-\left[\chi_{sw}\left(T,\phi_s^\beta\right)\phi_s^{2\beta}+\frac{\delta\chi_{sw}\left(T,\phi_s^\beta\right)}{\delta\phi_s^\beta}\phi_s^{2\beta}\left(1-\phi_s^\beta\right)\right]=0 \qquad (8)$$

$$v\left[+\left(1-\frac{v_S}{v_w}\right)\left(2-\phi_s^{\alpha}-\phi_s^{\beta}\right)\right]$$
$$+\left[\frac{v_s}{v_w}\,\chi_{sw}\,(T,\phi_s^{\alpha})(1-\phi_s^{\alpha})^2+\frac{v_s}{v_w}\phi_s^{\alpha}(1-\phi_s^{\alpha})^2\,\frac{\delta\chi_{sw}(T,\phi_s^{\alpha})}{\delta\phi_s^{\alpha}}\right]$$
$$+\left[\frac{v_s}{v_w}\,\chi_{sw}\left(T,\phi_s^{\beta}\right)\left(1-\phi_s^{\beta}\right)^2+\frac{v_s}{v_w}\phi_s^{\beta}\left(1-\phi_s^{\beta}\right)^2\,\frac{\delta\chi_{sw}\left(T,\phi_s^{\beta}\right)}{\delta\phi_s^{\beta}}\right]=0 \quad (9)$$

The critical point is given by the following conditions:

$$\frac{\delta^2\left(\frac{F}{RT}\right)}{\delta\phi_s^2}=\frac{\delta^3\left(\frac{F}{RT}\right)}{\delta\phi_s^3}=0 \qquad (10)$$

CHAPTER 4

RESULTS AND DISCUSSION

4.1) REGRESSION PARAMETERS

Table 1 – Unknown Parameters for N = 3

	NaCl	**LiCl**	**Li_2SO_4**	**$MgSO_4$**	**$CaCl_2$**
a	79.25810001	-13416.83325	1805.607702	41812.72232	6917.205725
b	0.392577746	-13655.82569	-1.52985731	-1710403.759	-2045.137046
c	406.7499327	1438.11892	-162.818885	-124710.7606	-40191.75976
d	79.25813745	-17830.20198	1804.459355	25437.18659	8303.19844
e	0.393322704	1813.197152	-1.53831223	-1693135.758	-6.0165132628
f	406.7499327	1840.796406	-314.8768451	114649.0606	38116.51935
g	-461.7558628	216895.324	-16834.84598	-49205.42678	-55686.377
h	-1.299947942	15369.79572	-5.859168109	3900142.407	1578.732542
i	-2712.455354	-25218.75124	-5264.96013	5674.916688	7106.784597
j	-286.6609284	-200587.7443	-73341.05538	-57730.37146	109013.936
k	-0.825744651	-92.36609842	-3.144404132	75602.14676	-3999.432868
l	-1677.795905	6619.358175	4942.140603	4823.346649	-22960.88857

Table 2 – Unknown Parameters for N = 4

	NaCl	**LiCl**	**Li_2SO_4**	**$MgSO_4$**	**$CaCl_2$**
a	-0.212294839	-8475.14118	1583.531513	735.2502247	8261.720861
b	-335.4371663	1.951984408	-1.523361753	-0.791706136	0.574569962
c	10342.4994	11063.71503	335.0484774	-175.5402835	-2205.145069
d	-0.207433846	-8762.679933	1586.790475	735.2499917	8514.638057
e	-323.2401916	1.945589229	-1.521177232	-0791302324	0.57414814
f	-35421.30669	-5249.227446	309.9047436	-175.5427682	637.5750879
g	-4.150170132	139528.488	-21459.34288	6263.204201	-64139.42738
h	357.187306	-2.140533011	-5.649620842	-1.789600289	-1.661789026
i	3024.992372	-42267.20539	-16192.5649	-3417.892075	1822.071307
j	-1.176700102	-28829.39158	-51230.10337	-10121.37875	119035.627
k	9279.052789	-3.087335404	-3.048952414	-1.185368643	-1.257998805
l	0	49056.73421	52595.85194	2229.518494	-1687.598625
m	102073.3323	-139583.3918	-4265.223202	-1750.261638	5734.631344
n	-0.353976317	-2.475147526	-1.159889792	-0.569492703	-0.617783764
o	-33101.67039	-35949.50214	-78519.87037	-6399.459638	-28747.96172

4.2) PARITY PLOT GRAPHS

1. NaCl

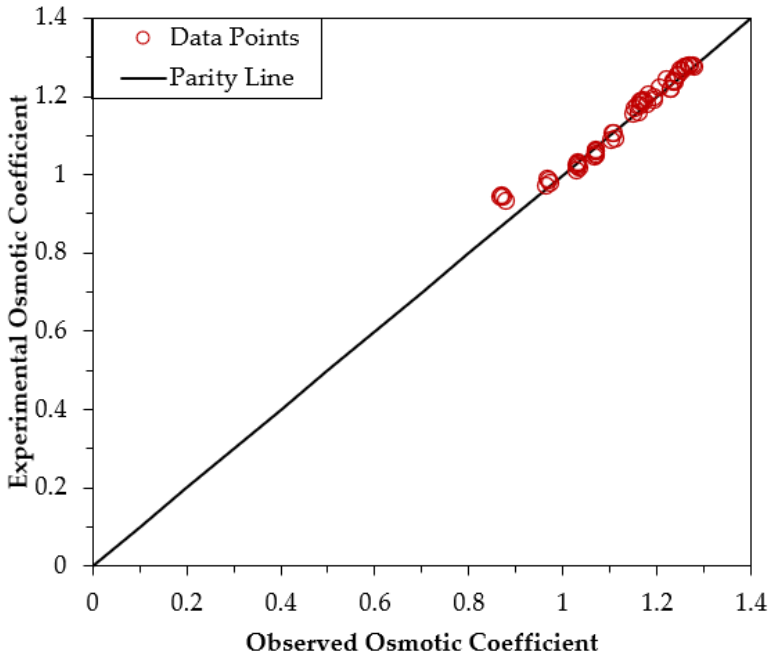

Fig 1. Parity plot of NaCl for N=3

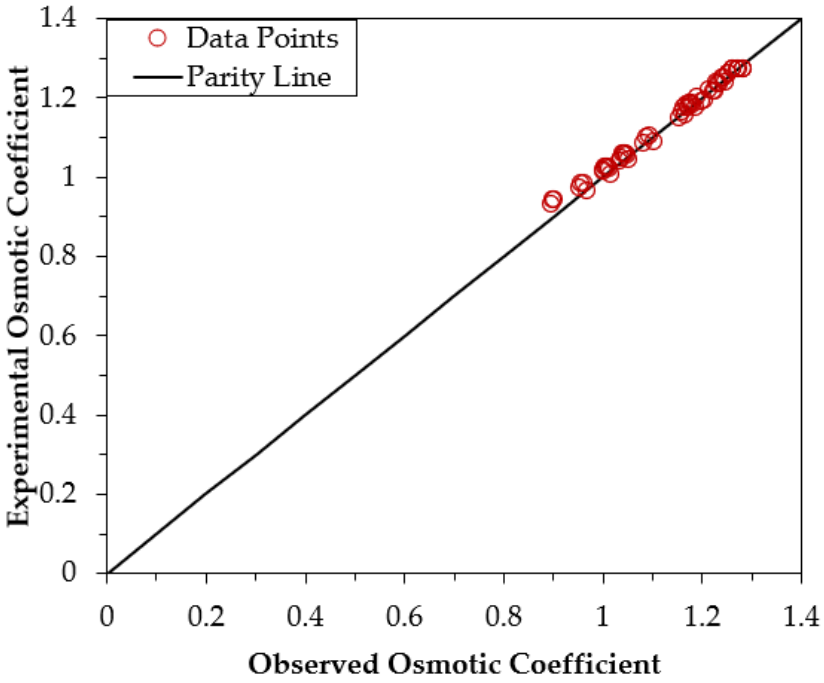

Fig 2. Parity plot of NaCl for N=4

2. LiCl

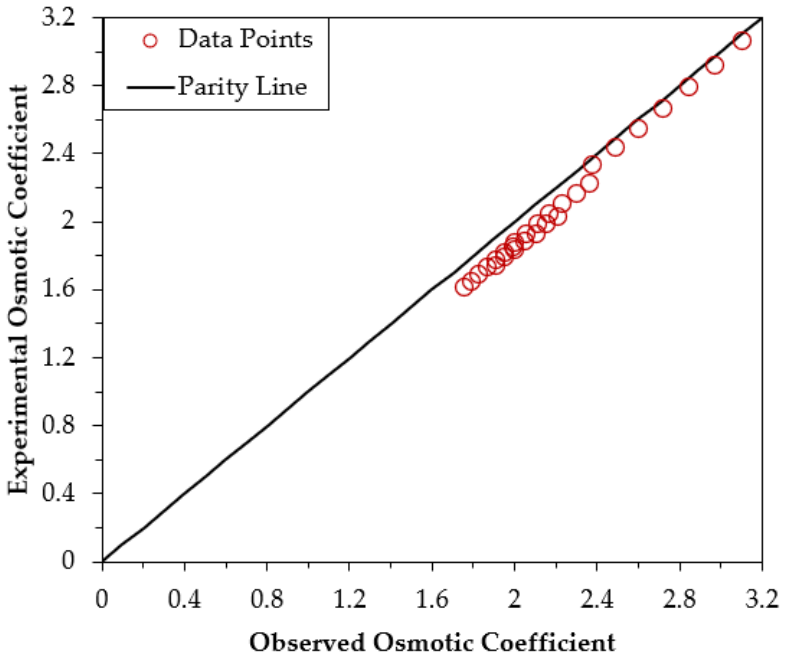

Fig 3. Parity plot of LiCl for N=3

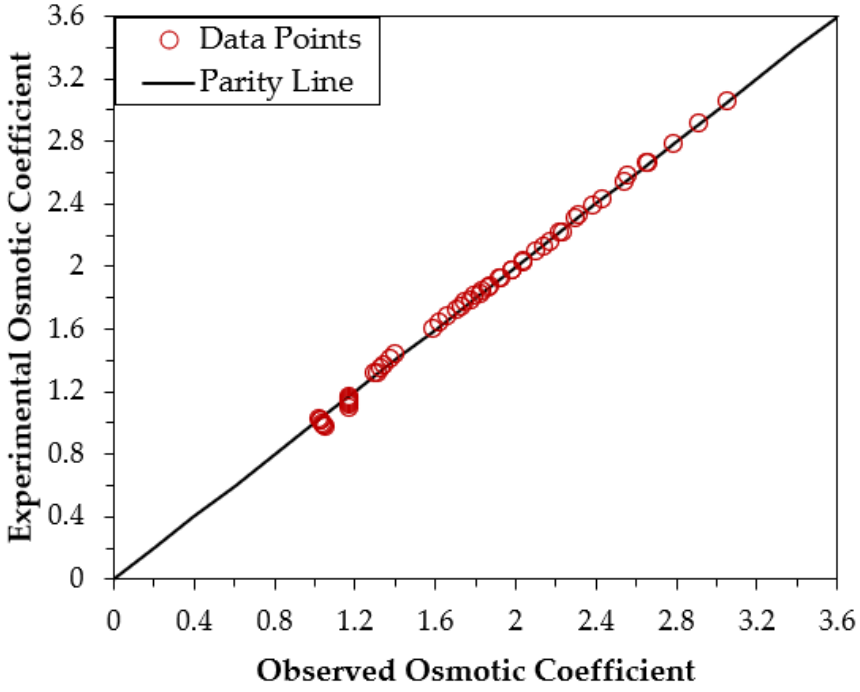

Fig 4. Parity plot of LiCl for N=4

3. $CaCl_2$

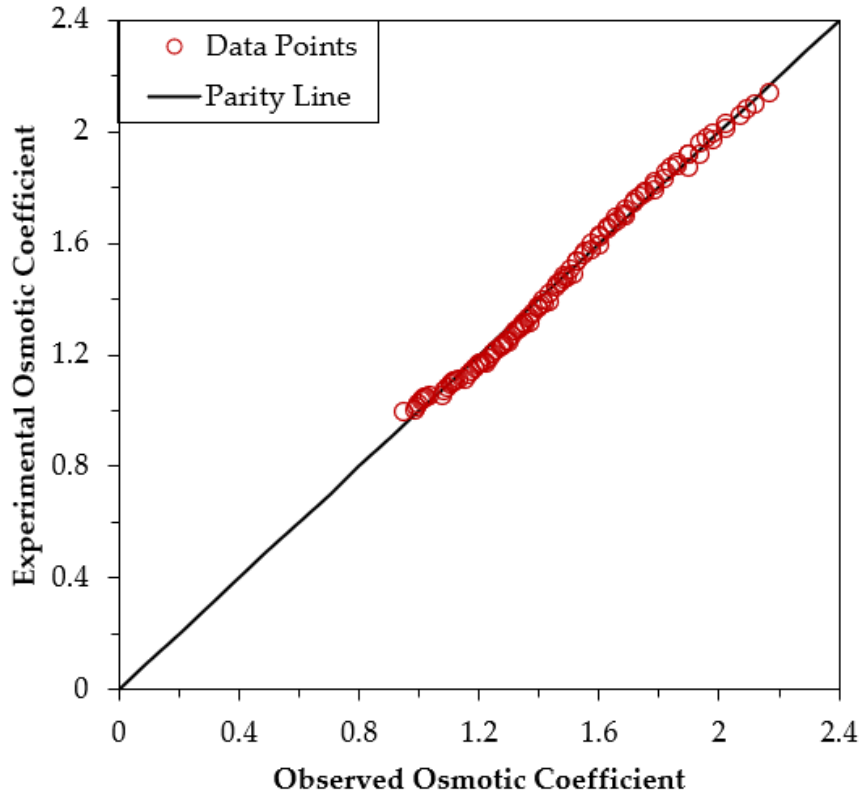

Fig 5. Parity plot of $CaCl_2$ for N=3

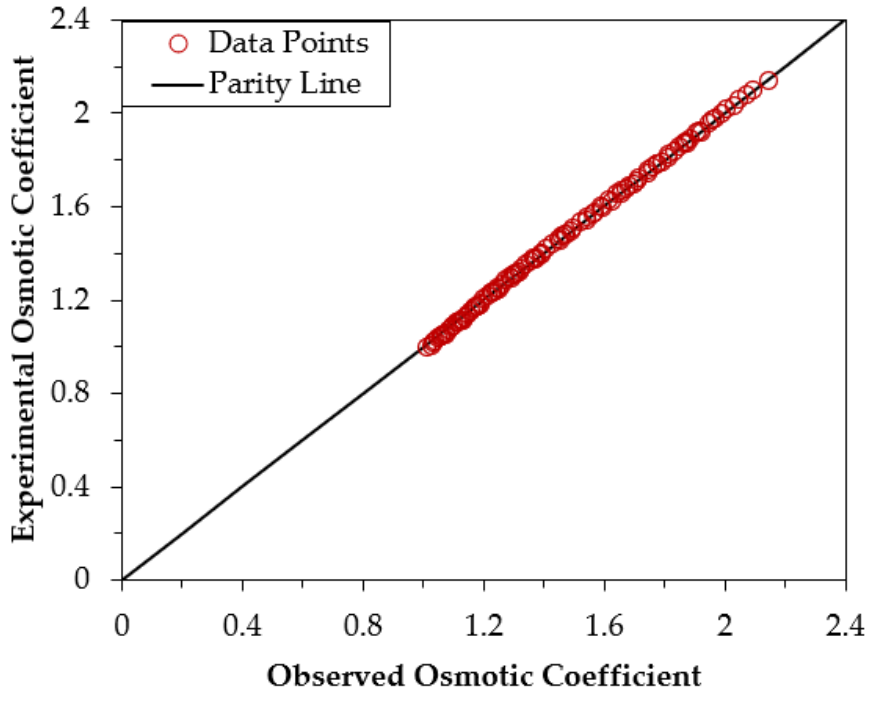

Fig 6. Parity plot of $CaCl_2$ for N=4

4. Li_2SO_4

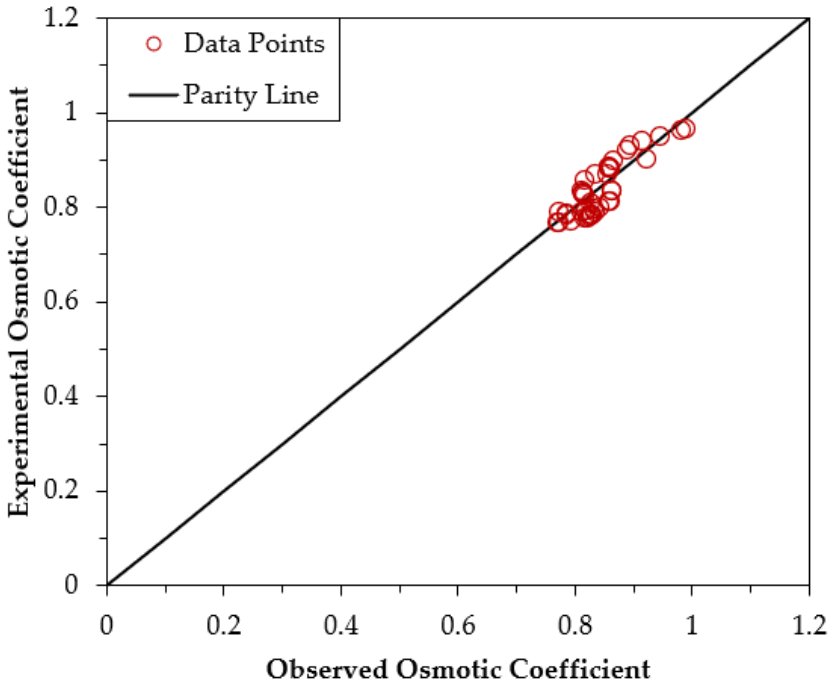

Fig 7. Parity plot of Li_2SO_4 for N=3

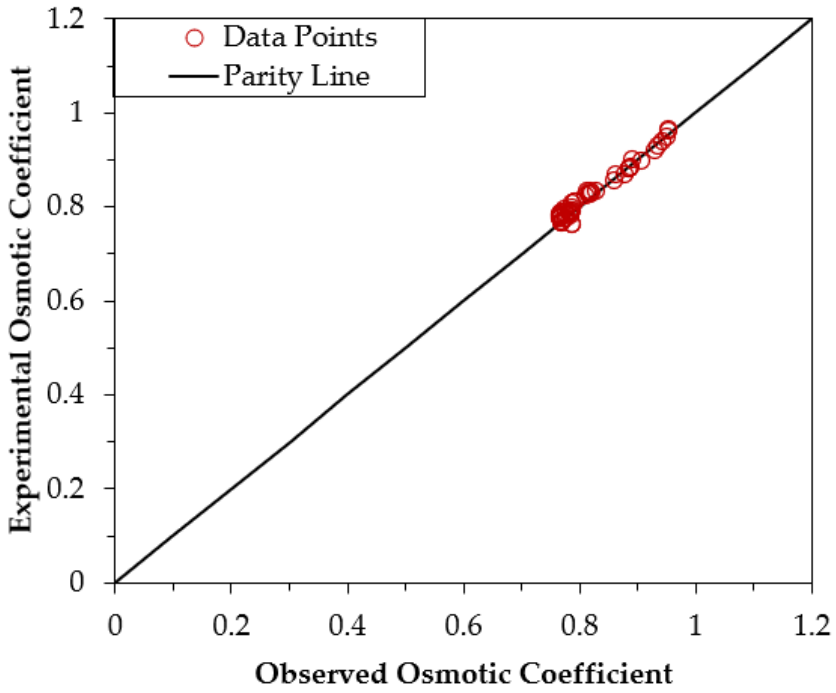

Fig 8. Parity plot of Li_2SO_4 for N=4

5. $MgSO_4$

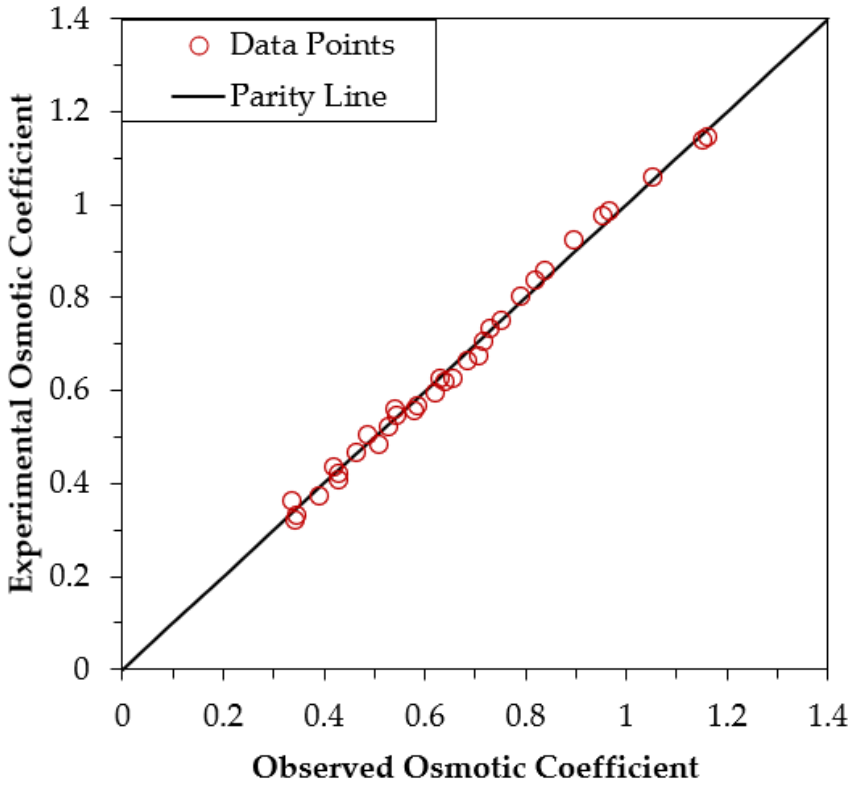

Fig 9. Parity plot of $MgSO_4$ for N=3

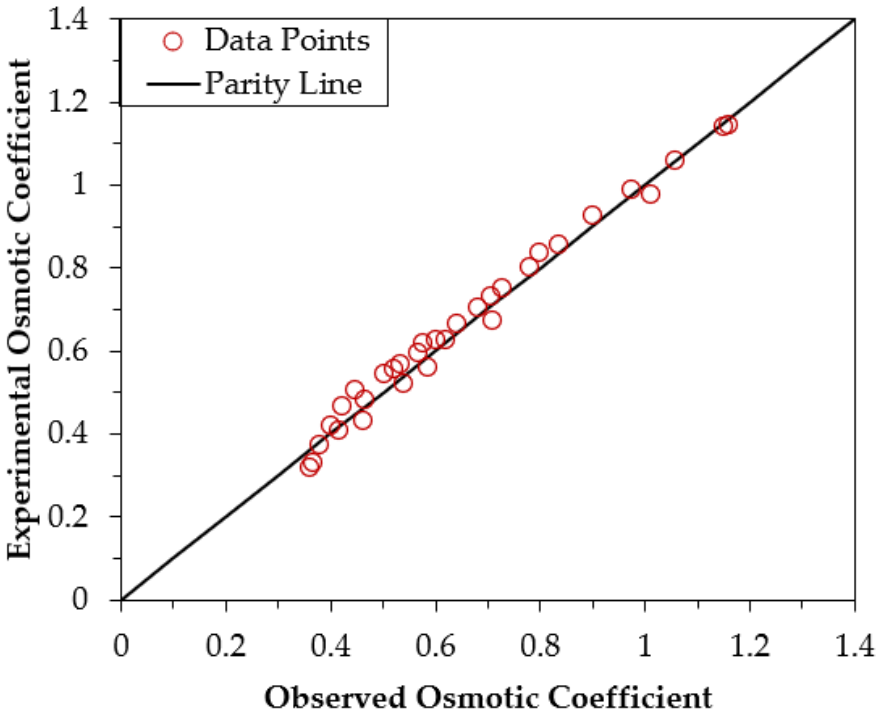

Fig 10. Parity plot of $MgSO_4$ for N=4

4.3) PHASE DIAGRAM GRAPHS

1. NaCl

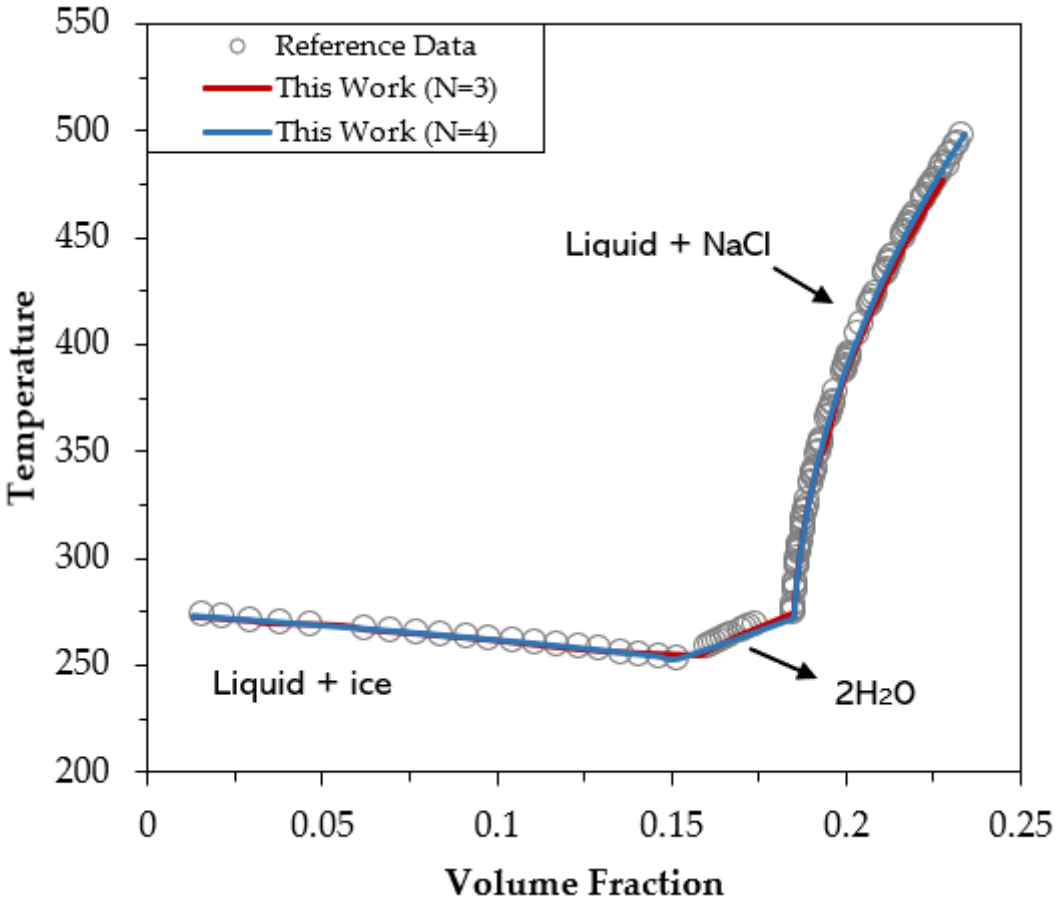

Fig 11. Temperature vs Volume fraction of NaCl

Fig 11 represents the phase diagram of NaCl + H_2O system. The diagram shows areas that represent a particular mixture of salt of NaCl and water at a given temperature. The point at a temperature of 253K is called eutectic point, which is the lowest temperature at which a liquid phase is stable at a given pressure. It's when a solid solute, a solid solvent, and a liquid mixture all exist in the same phase. The eutectic point is also known as the eutectic temperature and is the lowest possible melting point over all of the mixing ratios of the constituents. The temperature range of 253K to 272K represents the NaCl.$2H_2O$ + liquid system which means that you have a rock salt crystal with water molecules as a kind of dissolved impurity ($2H_2O$ molecules occupying the place of one NaCl unit), whereas the temperature this represents the NaCl + liquid system. The complete solid – liquid equilibrium data is traced almost exactly with experimental values for both N=3 and N=4 lines.

2. LiCl

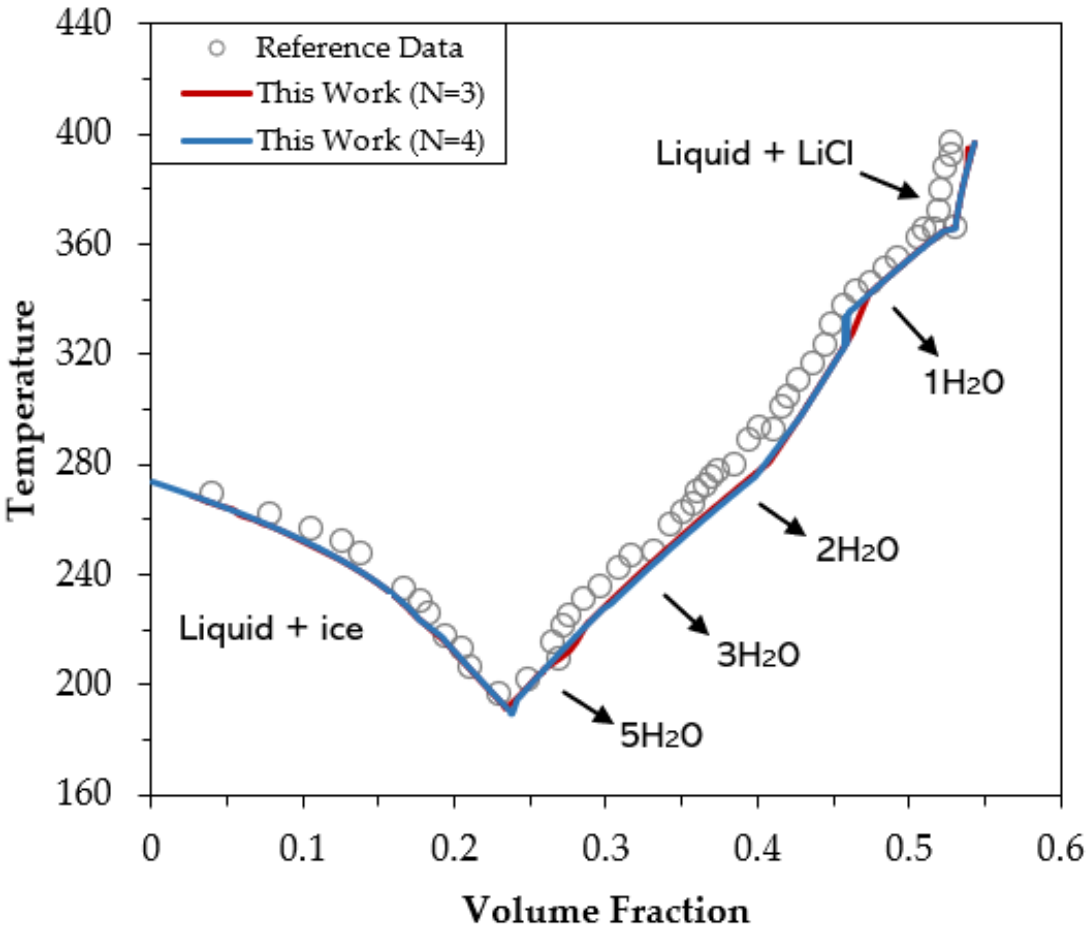

Fig 12. Temperature vs Volume fraction of LiCl

Fig 12 represents the phase diagram for LiCl + H_2O system. Besides anhydrous LiCl, there exist four solid lithium chloride hydrates, with respectively 1, 2, 3, and 5 water molecules. These salts are extremely soluble in water. For example, the solubility of the monohydrate LiCl.H_2O is about 20 mol/kg of H_2O in pure water at 273 K. At the eutectic temperature of the LiCl + H_2O system (199 K), which is one of the lowest of all alkali + water or alkaline earth + water systems, the stable solid is the pentahydrate LiCl.$5H_2O$. Despite this very low temperature, the concentration of the saturated solutions is very high, 24% volume fraction of salt at the eutectic. The calculated liquidus in the LiCl + H_2O system showed good agreement with the experimental results for both N=3 and N=4 lines.

3. $CaCl_2$

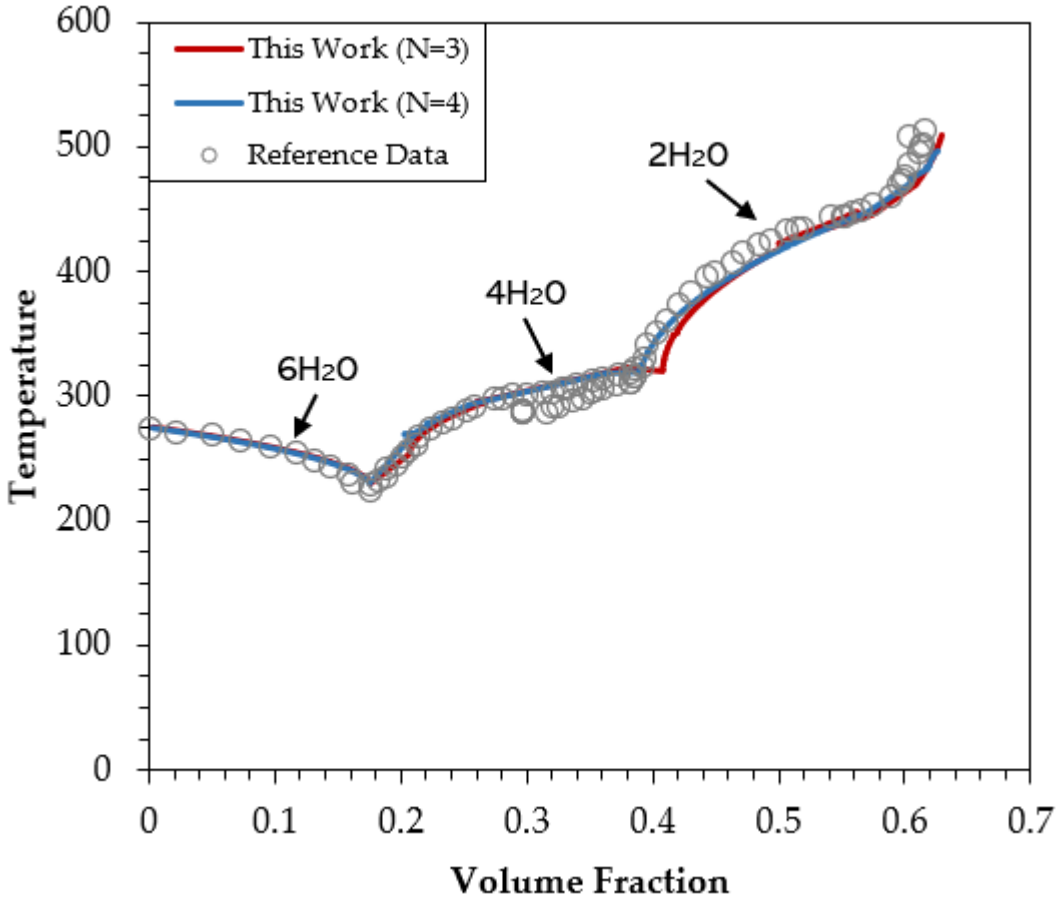

Fig 13. Temperature vs Volume fraction of $CaCl_2$

Fig 13 represents the phase diagram for $CaCl_2$ + H_2O system. Phases at equilibrium for the chemical system $CaCl_2$ + H_2O are shown as a function of volume fraction of $CaCl_2$ salt and temperature. There are three solid $CaCl_2$ hydrates of 2, 4 and 6. In which $CaCl_2.6H_2O$ and $CaCl_2.2H_2O$ occur naturally and have mineral names which are called as antarctictites and sinjarites respectively. The eutectic point of this system is around 223.5K. Till the volume fraction of 0.4, our model showed an excellent agreement with the experimental data for both N=3 and N=4 lines, above with N=4 line tried to trace almost with the experimental data where N=3 line showed a slight deviation till volume fraction of 0.56.

4. Li_2SO_4

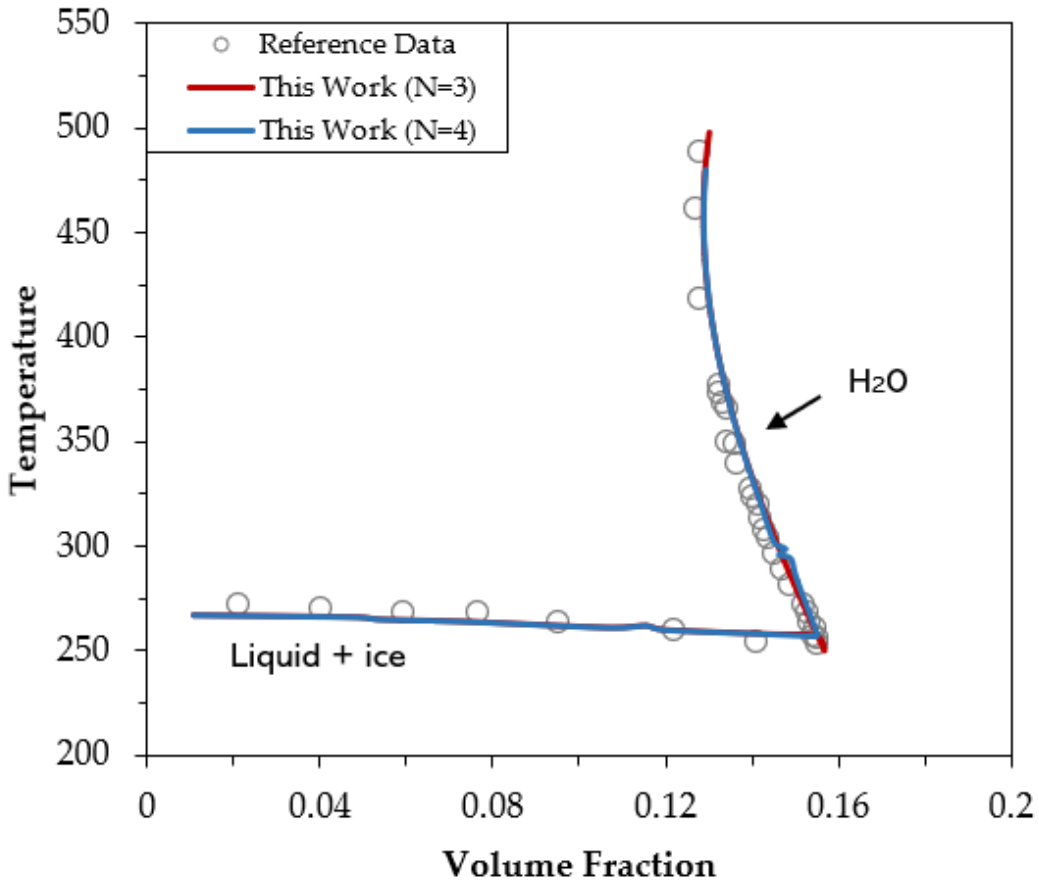

Fig 14. Temperature vs Volume fraction of Li_2SO_4

Fig 14 represents the phase diagram of $Li_2SO_4 + H_2O$ system. This system depicted a simple curve. There is a slight increase in the solubility of Li_2SO_4 till the eutectic point of around 250K. Here there exist only one form of hydrate salt which is $Li_2SO_4.H_2O$. Our model made an excellent argument in terms of tracing the experimental values with our model values for both N=3 and N=4.

5. $MgSO_4$

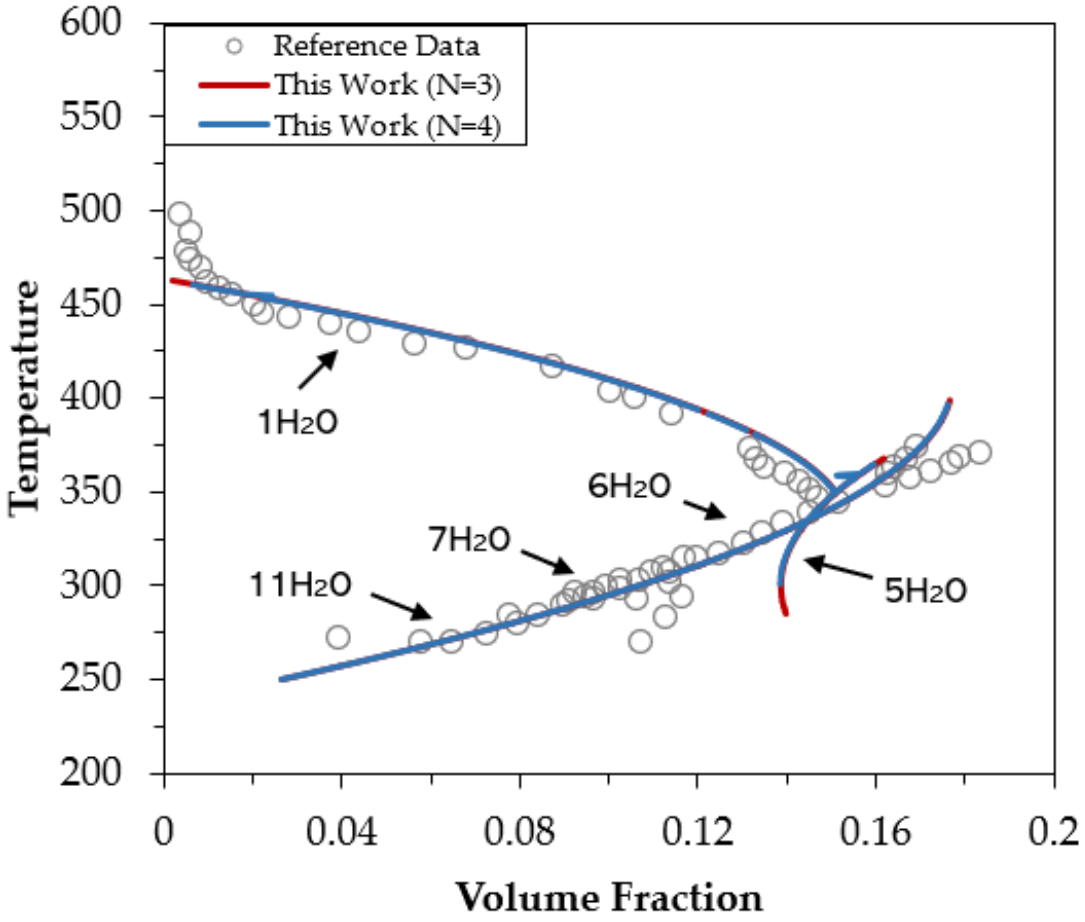

Fig 15. Temperature vs Volume fraction of $MgSO_4$

Fig 15 represents the phase diagram of $MgSO_4 + H_2O$ system. The phase diagram for the $MgSO_4 + H_2O$ system is more complex because there are more than three phases that can exist. In addition to the solid, liquid, and gas phases, there are also several hydrate phases. Those different hydrate include a count of 1, 4, 5, 6, 7 and 11 molecules of H_2O. The phase diagram for the $MgSO_4 + H_2O$ system is useful for understanding the behaviour of this system in different conditions. For example, the diagram can be used to determine the conditions at which magnesium sulphate heptahydrate will form or decompose. This information can be used in a variety of applications, such as the production of magnesium sulphate and the desalination of water. Our model gave an excellent result of aligning with the experimental values for both N=3 and N=4. There is a slight deviation from the experimental values in between the volume fraction of 0.0036 till 0.011.

The model calculated phase diagrams of the Li_2SO_4+H_2O, NaCl+ H_2O, LiCl+ H_2O, $MgSO_4$+ H_2O and $CaCl_2$+ H_2O systems compared with solubility data reported in literature are plotted in the above graphs. The unknown parameters of the equation 5, which helped us achieve this were tabulated in the table 1 and 2. There were 12 and 15 unknown parameters were there for n=3 and n=4 respectively. As shown in above graphs, most of the solid-liquid equilibria data, i.e. the points on the solubility curve, can be reproduced well using the present comprehensive thermodynamic models. Ice solubility data for all these systems can be accurately predicted even though they were not used in model parameterization.

For NaCl, we were able to exactly map the data against the literature work. We can be able to observe minor changes in the temperature with an increase in the volume fraction from 0.02 to 0.15, above with there is a sudden increase in the temperature from 250K till 550K. This shift indicates the reduction in the water molecules attached with NaCl from ice, $NaCl.2H_2O$ to $NaCl.H_2O$. Similarly, our model well performed in tracing the graphs for Li_2SO_4 as shown in the above graphs. There was a slight deviation for $CaCl_2$ between the volume fraction of 0.42 to 0.53, which is a region of 2 H_2O molecules attached with it.

The available solubility data of $MgSO_4$ between the volume fraction of salt hydrate from 0.10 to 0.12 and 0.16 till 0.18 are kind of scattered and hard to give a critical evaluation on their reliability. Nevertheless, the model result was not affected by the scattered experimental data significantly in those volume fraction of salt hydrate but gave a regular variation. In the system of $MgSO_4$+ H_2O, the solubilities of metastable solid phases $MgSO_4 \cdot 4\ H_2O$ and $MgSO_4 \cdot 5\ H_2O$ were also tried to simulate except for those stable solid phases. $MgSO_4 \cdot 11\ H_2O$ was recognized as stable phase at low temperature, although the solid phase corresponding to its solubilities in early literature were determined as $MgSO_4 \cdot 12\ H_2O$.

The difference of eutectic temperature of $Li_2SO_4 \cdot\ H_2O$ +ice between the present model predicted value and that recommended by Linke [76] and Sohr et al. [75] is about 2 K. According to the critical evaluation of Sohr et al. [75], the uncertainty of the eutectic temperature is 2 K. So, in such an uncertainty range, the present model result agrees with the recent recommendation of Sohr et al. [75] well. The eutectic composition of this invariant point predicted from the present model agree with those reported by Linke [76] and Sohr et al. [75] in absolute error 0.6% weight percentage, which is in accordance with the uncertainty reported by Sohr et al. [75] recently.

The parity plot for each salt hydrates explains how well this model has predicted its output compared to the Literature data. Our model almost traced its value with the literature value and gave us the error deviation of less than 4%.

REFERENCES

1) Belaïd F. Understanding the spectrum of domestic energy consumption: empirical evidence from France. Energy Policy 2016;92:220–33
2) VROM. Tech rep; 2016. http://www.publicatiereeksgevaarlijkestoffen.nl/
3) Zondag H, Kikkert B, Smeding S, Boer De R, Bakker M. Prototype thermochemical heat storage with open reactor system. Appl Energy 2013;109:360–5.
4) Schmidt M, Szczukowski C, Roßkopf C, Linder M, Wörner A. Experimental results of a 10 kW high temperature thermochemical storage reactor based on calcium hydroxide. Appl Therm Eng 2014;62(2):553–9.
5) Gaeini M, Zondag H, Rindt C. Effect of kinetics on the thermal performance of a sorption heat storage reactor. Appl Therm Eng 2016;102:520–31.
6) Knoll C, Müller D, Artner W, Welch J, Werner A, Harasek M, et al. Probing cycle stability and reversibility in thermochemical energy storage – CaC2O4 H2O as perfect match? Appl Energy 2017;187:1–9.
7) N'Tsoukpoe K, Schmidt T, Rammelberg H, Watts B, Ruck W. A systematic multi step screening of numerous salt hydrates for low temperature thermochemical energy storage. Appl Energy 2014;124:1–16.
8) Hermans, J, Energy Survival Guide; 2008.
9) Trausel, F et al., "A review on the properties of salt hydrates for thermochemical storage", SHC 2013, International Conference on Solar Heating and Cooling for Buildings and Industry September 23-25, 2013, Freiburg, Germany, Energy Procedia; 2014
10) Cook J, Nuccitelli D, Green SA, Richardson M, Winkler B, Painting R, et al. Quantifying the consensus on anthropogenic global warming in the scientific literature. Environ Res Lett 2013;7. http://dx.doi.org/10.1016/j. enpol.2014.06.003
11) Rafiq S, Salim R, Nielsen I. Urbanization, openness, emissions and energy intensity: a study of increasingly urbanized emerging economies. Energy Econ 2016;56:20–8. http://dx.doi.org/10.1016/j.eneco.2016.02.007.
12) Blarke MB, Lund H. The effectiveness of storage and relocation options in renewable energy systems. Renew Energy 2008;33:1499–507. http://dx.doi.org/10.1016/j.renene.2007.09.001.
13) Blarke MB, Jenkins BM. SuperGrid or SmartGrid: competing strategies for large-scale integration of intermittent renewables? Energy Policy 2013;58:381–90. http://dx.doi.org/10.1016/j.enpol.2013.03.039.
14) Kalaiselvam S, Parameshwaran R. Energy storage. Therm. energy storage Technol Sustain - Syst Des Assess Appl. Elsevier Inc; 2014. p. 21–56. http://dx.doi.org/10.1016/B978-0-12-417291-3.00002-5.
15) Kalaiselvam S, Parameshwaran R. Seasonal thermal energy storage. Therm energy storage Technol Sustain - Syst Des Assess Appl. Elsevier Inc; 2014. p. 145–62. http://dx.doi.org/10.1016/B978-0-12-417291-3.00007-4.
16) Gao L, Zhao J, Tang Z. A review on borehole seasonal solar thermal energy storage. Energy procedia, vol. 70. Elsevier B.V; 2015. p. 209–18. http://dx.doi.org/10.1016/j.egypro.2015.02.117.

17) Pinel P, Cruickshank Ca, Beausoleil-Morrison I, Wills A. A review of available methods for seasonal storage of solar thermal energy in residential applications. Renew Sustain Energy Rev 2011;15:3341–59. http://dx.doi.org/10.1016/j.rser.2011.04.013.
18) Yu N, Wang RZ, Wang LW. Sorption thermal storage for solar energy. Prog Energy Combust Sci 2013;39:489–514. http://dx.doi.org/10.1016/j. pecs.2013.05.004 Review.
19) Xu J, Wang RZ, Li Y. A review of available technologies for seasonal thermal energy storage. Sol Energy 2013;103:610–38. http://dx.doi.org/10.1016/j.solener.2013.06.006.
20) Aydin D, Casey SP, Riffat S. The latest advancements on thermochemical heat storage systems. Renew Sustain Energy Rev 2015;41:356–67. http://dx.doi.org/10.1016/j.rser.2014.08.054.
21) Ervin G. Solar heat storage using chemical reactions. J Solid State Chem 1977;22:51–61. http://dx.doi.org/10.1016/0022-4596(77)90188-8
22) Ding Y, Riffat S. Thermochemical energy storage technologies for building applications: a state-of-the-art review. Int J Low-Carbon Technol 2012;8:106–16. http://dx.doi.org/10.1093/ijlct/cts004.
23) P.S. Song, Y. Yao, Thermodynamics and phase diagram of the salt lake brine system at 298.15 K: V. Model for the system $Li^{þ}$, Naþ, $K^{þ}$, $Mg^{2þ}$/Cl , SO_4^{2} –H_2O and its applications, CALPHAD 27 (2003) 343–352.
24) P.S. Song, Y. Yao, Parameters of Pitzer model for the salt lake brine system and their applications I. Applications in physical chemistry for the system $Li^{þ}$, $Na^{þ}$, $K^{þ}$, $Mg^{2þ}$/Cl , SO_4^{2} –H_2O, J. Salt Lake Res. 11 (3) (2003) 1–7.
25) P.S. Song, Y. Yao, Parameters of Pitzer model for the salt lake brine system and their applications II. Prediction of solubilities in the system $Li^{þ}$, $Na^{þ}$, $K^{þ}$, $Mg^{2þ}$/Cl , SO_4^{2} –H_2O, J. Salt Lake Res. 11 (4) (2003) 1–11.
26) P.S. Song, Y. Yao, Parameters of Pitzer model for the salt lake brine system and their applications III. Applications in process technology in the system $Li^{þ}$, $Na^{þ}$, $K^{þ}$, $Mg^{2þ}$/Cl , SO_4^{2} –H_2O, J. Salt Lake Res. 12 (3) (2004) 1–10.
27) X. Yin, Q.X. Li, Y.P. Wan, B.H. Li, D.W. Zeng, Comparison of thermodynamic models in high-solubility saltþH_2O systems I: binary systems, Acta Chim. Sin. 66 (2008) 1815–1826.
28) Holmes, H.F., Baes Jr., C.F., Mesmer, R.E.: Isopiestic studies of aqueous solutions at elevated temper atures I. KCl, $CaCl_2$, and $MgCl_2$. J. Chem. Thermodyn. **10**, 983–996 (1978)
29) Clegg, S.L., Pitzer, K.S., Brimblecombe, P.: Thermodynamics of multicomponent, miscible, ionic solutions. Mixtures including unsymmetrical electrolytes. J. Phys. Chem. **96**, 9470–9479 (1992)
30) Clegg, S.L., Pitzer, K.S.: Thermodynamics of multicomponent, miscible, ionic solutions: general ized equations for symmetrical electrolytes. J. Phys. Chem. **96**, 3513–3520 (1992)

31) Ghalami-Choobar, B., Mossayyebzadeh-Shalkoohi, P.: Activity coefcient measurements and ther modynamic modeling of ($CaCl_2$+ l-alanine + water) system based on potentiometric determination at *T* = (298.2, 303.2, and 308.2) K. J. Chem. Eng. Data **60**, 2879–2894 (2015)
32) Ghalami-Choobar, B., Sayyadi-Nodehi, F.: Thermodynamic study of the (NaCl + serine + water) mixtures using potentiometric measurements at *T* = (298.2 and 303.2) K. Fluid Phase Equilib. **380**, 48–57 (2014)
33) Ghalami-Choobar, B., Mirzaie, S.: Thermodynamic study of (KCl + proline + water) system based on potentiometric measurements at *T* = (298.2 and 303.2) K. J. Mol. Liq. **169**, 124–129 (2012)
34) Ali, H., Sarkisian, E.: Thermodynamics of vapor–liquid equilibrium in mixed solvent electrolyte sys tems. Sci. Iran **5**, 67–81 (1998)
35) Haghtalab, A., Vera, J.: A nonrandom factor model for the excess Gibbs energy of electrolyte solu tions. AIChE J. **34**, 803–813 (1988)
36) J. Berthet, J.J. Counioux, Thermochimica Acta 194 (1992) 137.
37) X. Yin, Q.X. Li, Y.P. Wan, B.H. Li, D.W. Zeng, Comparison of thermodynamic models in high-solubility saltþH_2O systems I: binary systems, Acta Chim. Sin. 66 (2008) 1815–1826.
38) Sures, D.J.; Serapian, S.A.; Kozma, K.; Molina, P.I.; Bo, C.; Nyman, M. Electronic and relativistic contributions to ion-pairing in polyoxometalate model systems. *Phys. Chem. Chem. Phys.* **2017**, *19*, 8715–8725. [CrossRef] [PubMed]
39) Akopov, E. K., 1962, Polytherms of solubility in the system LiCl-KCl-H_2O: Zhurnal Neorganicheskoi khimii (Russian Journal of Inorganic Chemistry), v. 7, p. 385–389.
40) Applebey, M., and Cook, R., 1938, The transition temperatures of lithium chloride hydrates: Journal of the Chemical Society, p. 547.
41) Wei, Z., Li, D., Hu, W., Analysis and Research on Regeneration Method and Device of Solar Dehumidification Solution, District Heating, 2014, 03(1), pp. 16-19.
42) Wen, X., Cao, X., Yu, P., Energy-saving analysis and experimental study of a new heat-source tower solution regeneration system, CIESC Journal, 2017, 12(5), pp. 35-39
43) Cheng, Q., Zhang, X., Performance Analysis of a New PV/T Desiccant Regeneration System, Acta Energiae Solaris Sinica, 2015, 36(7), pp. 1616-1621
44) Misha S, Mat S, Ruslan M H and Sopian K. Review of solid/liquid desiccant in the drying applications and its regeneration methods, Renewable and Sustainable Energy Reviews, 2012, 16(7), pp. 4686-4707
45) Tokunaga, T. K. *et al.* Water saturation relations and their difusion-limited equilibration in gas shale: Implications for gas fow in unconventional reservoirs. *Water Resour. Res.* **53**, 9757–9770 (2017).
46) A new method for production data analysis in shale gas reservoirs. *J. Nat. Gas Sci. Eng.* **56**, 368–383 (2018).
47) Guo, W. *et al.* Shale favorable area optimization in coal-bearing series: a case study from the Shanxi Formation in Northern Ordos Basin, China. *Energ. Explor. Exploit.* **36**(5), 1295–1309 (2018).

48). Yuan, B., Zheng, D., Moghanloo, R. G. & Wang, K. A novel integrated workfow for evaluation, optimization, and production predication in shale plays. *Int. J. Coal Geol.* **180**, 18–28 (2017).
49). Shen, W. J., Xu, Y. M., Li, X. Z., Huang, W. G. & Gu, J. R. Numerical simulation of gas and water fow mechanism in hydraulically fractured shale gas reservoirs. *J. Nat. Gas Sci. Eng.* **35**, 726–735 (2016).
50) Fisch N, Bodmann M, Kühl L, Saße C and Schnürer., H, Wärmespeicher. BINE Informationsdienst, 4th edition, Bonn 2005.
51) van Essen V M, Cot Gores J, Bleijendaal L P J, Zondag H A, Schuitema R and van Helden W G J Characterisation of salt hydrates for compact seasonal thermochemical storage, Proceedings of the ASME 3rd International Conference on Energy Sustainability, July 19-23, San Francisco, California, USA, 2009.
52) Schaube F, Wörner A and Müller-Steinhagen H, High temperature heat storage using gas-solid reactions. Conference proceedings of the EFFSTOCK 11th International Conference on Energy Storage, June 14-17, Stockholm, Schweden, 2009.
53) Opel O, Rammelberg H U, Gérard M and Ruck W, Thermochemical Storage Materials Research - TGA/DSC-Hydration Studies, prepared for International Conference on Sustainable Energy Storage 2011, February 21.-24., Belfast, Ireland 2011
54) Rammelberg H U, Opel O, Ross S, Ruck W, Hydration and Dehydration of CaO/ $Ca(OH)_2$ and $CaCl_2$ / $CaCl_2$ * 6 H_2O– TGA/ DSC studies, 6th International Renewable Energy Storage Conference IRES 2011, 28-30 November 2011, Berlin, Germany.
55) Rard, J.A., Clegg, S.L., Palmer, D.A.: Isopiestic determination of the osmotic coefficients of Na_2SO_4(aq) at 25 and 50 °C, and representation with ion interaction (Pitzer) and mole fraction thermodynamic models. J. Solution. Chem. **29**, 1–49 (2000).
56) Palmer, D.A, Archer, D.G., Rard, J.A.: Isopiestic determination of the osmotic and activity coefficients of K_2SO_4(aq) at the temperatures 298.15 K and 323.15 K, and revision of the thermodynamic properties of the K_2SO_4 + H_2O system. J. Chem. Eng. Data **47**, 1425–1431 (2002).
57) Holmes, H.F., Mesmer, R.E.: Thermodynamics of aqueous solutions of the alkali metal sulfates. J. Solution Chem. **15**, 495–517 (1986).
58) Palmer, D.A., Rard, J.A., Clegg, S.L.: Isopiestic determination of the osmotic and activity coefficients of Rb_2SO_4(aq) and Cs_2SO_4(aq) at T = (298.15 and 323.15) K, and representation with an extended ion-interaction (Pitzer) model. J. Chem. Thermodyn. **34**, 63–102 (2002).
59) W.F. Linke, A. Seidell (Eds.), Solubilities, Inorganic and Metal-Organic Compounds, American Chemical Society, Washington, DC, 1965.
60) D. Smith-Magovan, D. Garvin, V.B. Parker, R.L. Nutall, B.R. Staples, in: D. Garvin, V.B. Parker, H.J. White Jr. (Eds.), CODATA Thermodynamic Tables. Selections for Some Compounds of Calcium and Related Mixtures: A Prototype Set of Tables, Hemisphere, Washington, DC, 1987

61) D. Zeng, J. Zhou, J. Chem. Eng. Data 51 (2006) 315–321.
62) Lane, G.A. Phase-Change Materials for Energy-Storage Nucleation to Prevent Supercooling. *Sol. Energy Mater. Sol. Cells* **1992**, *27*, 135–160. [CrossRef]
63) Sharma, A.; Tyagi, V.V.; Chen, C.R.; Buddhi, D. Review on thermal energy storage with phase change materials and applications. *Renew. Sustain. Energy Rev.* **2009**, *13*, 318–345. [CrossRef]
64) Safari, A.; Saidur, R.; Sulaiman, F.A.; Xu, Y.; Dong, J. A review on supercooling of Phase Change Materials in thermal energy storage systems. *Renew. Sustain. Energy Rev.* **2017**, *70*, 905–919. [CrossRef]
65) Shahbaz, K.; AlNashef, I.M.; Lin, R.J.; Hashim, M.A.; Mjalli, F.S.; Farid, M.M. A novel calcium chloride hexahydrate-based deep eutectic solvent as a phase change materials. *Sol. Energy Mater. Sol. Cells* **2016**, *155*, 147–154.
66) . Kibria, M.A.; Anisur, M.R.; Mahfuz, M.H.; Saidur, R.; Metselaar, I.H. A review on thermophysical properties of nanoparticle dispersed phase change materials. *Energy Convers. Manag.* **2015**, *95*, 69–89. [CrossRef]
67) Ma, Y.; Lei, B.Y.; Liu, Y.C.; Wu, T. Effects of additives on the subcooling behavior of $Al_2(SO_4)_3{\cdot}18H_2O$ phase transition. *Appl. Therm. Eng.* **2016**, *99*, 189–194
68) He, Q.; Wang, S.; Tong, M.; Liu, Y. Experimental study on thermophysical properties of nanofluids as phase-change material (PCM) in low temperature cool storage. *Energy Convers. Manag.* **2012**, *64*, 199–205.
69) R. K. Sharma, P. Ganesan, V. V. Tyagi, and T. M. I. Mahlia, "Accelerated thermal cycle and chemical stability testing of polyethylene glycol (PEG) 6000 for solar thermal energy storage," Solar Energy Materials and Solar Cells, vol. 147, pp. 235–239, 2016.
70) Blarke MB, Lund H. The effectiveness of storage and relocation options in renewable energy systems. Renew Energy 2008;33:1499–507. http://dx.doi.org/10.1016/j.renene.2007.09.001.
71) Blarke MB, Jenkins BM. SuperGrid or SmartGrid: competing strategies for large-scale integration of intermittent renewables? Energy Policy 2013;58:381–90. http://dx.doi.org/10.1016/j.enpol.2013.03.039.
72) Kalaiselvam S, Parameshwaran R. Energy storage. Therm. energy storage Technol Sustain - Syst Des Assess Appl. Elsevier Inc; 2014. p. 21–56. http://dx.doi.org/10.1016/B978-0-12-417291-3.00002-5.
73) Reyes, J. R. M. D.; Parsons, R. V.; Hoemsen, R. Winter happens: The effect of ambient temperature on the travel range of electric vehicles. IEEE Trans. on Vehicular Technol. 2016, 65, 4016−4022.
74) Lin, R.; Taberna, P. L.; Fantini, S.; Presser, V.; Perez, C. R.;́ Malbosc, F.; Rupesinghe, N. L.; Teo, K. B.; Gogotsi, Y.; Simon, P. Capacitive energy storage from −50 to 100 C using an ionic liquid electrolyte. J. Phys. Chem. Lett. 2011, 2, 2396−2401.
75) Pielichowska, K.; Pielichowski, K. Phase change nanomaterials for thermal energy storage. In *Nanotechnology for Energy Sustainability*; Wiley: Hoboken, NJ, USA, 2017; pp. 459–484.

76) H. Lahmidi, S. Mauran, V. Goetz, Definition, test and simulation of a thermochemi cal storage process adapted to solar thermal systems, Sol. Energy 80 (7) (2006) 883–893
77) Comodi G, Bevilacqua M, Caresana F, Paciarotti C, Pelagalli L, Venella P. Life cycle assessment and energy-CO_2-economic payback analyses of renewable domestic hot water systems with unglazed and glazed solar thermal panels. Applied Energy. 2016;164:944-55.
78) M. Goldstein, Some physical chemical aspects of heat storage, in: UN Conf. New Sources Energy, Rome, vol. 3, 1961, 411–417.
79) G. Kipouros, D. Sadoway, The chemistry and electrochemistry of magnesium production, Adv. Molten Salt Chem. 6 (1987) 127–209.
80) R. Wheeler, G. Frost, A comparative study of the dehydration kinetics of several hydrated salts, Can. J. Chem. (1954) 546–561.
81) J. Mutin, G. Watelle, Y. Dusausoy, Study of a lacunary solid phase l – thermody namic crystallographic characteristics of its formation, J. Solid State Chem. 27 (1979) 407–421.
82) Mohamed, S.A.; Al-Sulaiman, F.A.; Ibrahim, N.I.; Zahir, M.H.; Al-Ahmed, A.; Saidur, R.; Yılba¸s, B.S.; Sahin, A.Z. A review on current status and challenges of inorganic phase change materials for thermal energy storage systems. *Renew. Sustain. Energy Rev.* **2017**, *70*, 1072–1089.
83) Li, G.; Zhang, B.; Li, X.; Zhou, Y.; Sun, Q.; Yun, Q. The preparation, characterization and modification of a new phase change material: $CaCl_2{\cdot}6H_2O$–$MgCl_2{\cdot}6H_2O$ eutectic hydrate salt. *Sol. Energy Mater. Sol. Cells* **2014**,
84) Pardo, P.; Deydier, A.; Anxionnaz-Minvielle, Z.; Rougé, S.; Cabassud, M.; Cognet, P. A review on high temperature thermochemical heat energy storage. *Renew. Sustain. Energy Rev.* **2014**, *32*, 591–610.
85) Hasnain, S.M. Review on sustainable thermal energy storage technologies, Part I: Heat storage materials and techniques. *Energy Convers. Manag.* **1998**, *39*,
86) Kwak, T.A.P., Hing Tan, T., 1981. The importance of $CaCl_2$ in fluid composition trends – evidence from the King Island (Dolphin) skarn deposit. Economic Geology 76 (4), 955–960.
87) Jiang, H.; Shin, W.; Ma, L.; Hong, J. J.; Wei, Z.; Liu, Y.; Zhang, S.; Wu, X.; Xu, Y.; Guo, Q.; Subramanian, M. A. A High-Rate Aqueous Proton Battery Delivering Power Below −78° C via an Unfrozen Phosphoric Acid. Adv. Energy Mater. 2020, 10, 2000968
88) Ramanujapuram, A.; Yushin, G. Understanding the Exceptional Performance of Lithium-Ion Battery Cathodes in Aqueous Electro lytes at Subzero Temperatures. Adv. Energy Mater. 2018, 8, 1802624
89) Tsai, W. Y.; Lin, R.; Murali, S.; Zhang, L. L.; McDonough, J. K.; Ruoff, R. S.; Taberna, P. L.; Gogotsi, Y.; Simon, P. Outstanding performance of activated graphene based supercapacitors in ionic liquid electrolyte from −50 to 80 C. Nano Energy 2013, 2, 403−411.
90) M. V. Mokhosoev and T. T. Got'manova, *Russ. J. Inorg. Chem.* **11**, 466 (1966). 2. H. Kimura and J. Kai, *Energy Conv. Mgmt.* **28**, 197 (1988).
91) J. E. Ricci, in *Molten Salt Chemistry*, M. Blander, ed. (Wiley/Interscience, New York, 1964), p. 255.
92) Lizana, J.; Chacartegui, R.; Barrios-Padura, A.; Ortiz, C. Advanced low-carbon energy measures based on thermal energy storage in buildings: A review. *Renew. Sustain. Energy Rev.* **2018**, *82*, 3705–3749.
93) Xu, J.; Wang, R.Z.; Li, Y. A review of available technologies for seasonal thermal energy storage. *Sol. Energy* **2014**, *103*, 610–638

94) Guarini, G.G.T.; Piccini, S. The dehydration of $Na_2S_2O_3 \cdot 5H_2O$ single crystals as studied by thermal analysis and optical microscopy. *J. Chem. Soc. Faraday Trans. 1 Phys. Chem. Condens. Phases* **1988**, *84*, 331
95) . Prieto, C.; Cooper, P.; Fernández, A.I.; Cabeza, L.F. Review of technology: Thermochemical energy storage for concentrated solar power plants. *Renew. Sustain. Energy Rev.* **2016**, *60*, 909–929.